PERIODICA POLYTECHNICA SER. MECH. ENG. VOL. 40, NO. 2, PP. 103-112 (1996)

RESIDUAL STRESSES IN THERMALLY LOADED SHRINK FITS[1]

Ádám KOVÁCS

Department of Technical Mechanics
Technical University of Budapest
H-1521 Budapest, Hungary
Fax: + 36 1463-3471
email: adamo@mm.bme.hu
Phone: + 36 1463-1367

Received: February 15, 1995

Abstract

This paper presents the results of comparative calculations by the finite element method of shrink fits having simple geometry on examination of the following aspects: yield criterion, hardening rule, temperature-dependence of the material parameters and the type of the uniaxial stress-strain curve. The necessary reference results for the comparison have been obtained by using partly analytical methods published by the author and others, partly the general purpose commercial finite element code COSMOS. The most significant difference has been detected at temperature-dependent material parameters.

Keywords: residual stress, shrink fit, thermoelasto-plasticity.

1. Introduction

Shrink fit is a simple device, produced from two cylindrical parts — sometimes of different materials — , which transfers axial force or torque. The loading transmission becomes possible without any adhesive, through only the solid contact of the parts due to the original interference to remove during the assemblage.

The scope of the present paper is the determination of the residual stress-state and, consequently, the transferable force or torque in shrink fits due to cyclic thermal loading after the assemblage assuming elastic-plastic deformations. There have been published several analytical methods applicable to the calculation of stresses due to the assemblage (e. g. KOLLMANN, 1978, Gamer and LANCE, 1982, KOLLMANN and ÖNÖZ, 1983, MACK, 1986). The first step towards the quantitative analysis of residual stresses in shrink fits after the assemblage was made by LIPPMANN (1992). His derivation was later generalized by KOVÁCS (1991 and 1994a). All these methods take, however, several presuppositions and negligences.

[1]This work has been financially supported by OTKA 5-814

Such assumptions are e.g. the Tresca yield criterion and its associated flow rule, a simple hardening rule (linear or exponential), the negligence of the temperature-dependence of material parameters, etc. By the use of the general purpose finite element code COSMOS it is possible to examine whether the assumptions mentioned permit only a rough approximation or, on the other hand, which parameters have the greatest influence on the residual stress state. In the comparison it is now important the mechanical model and not the effect of the different heat boundary conditions or the sophisticated computing methods related to the finite element method.

The effect of the following parameters on the residual stress state has been analyzed:

- yield criterion (Tresca or von Mises type);
- hardening rule (any, isotropic, anisotropic);
- temperature dependence of the material parameters (Young modulus, linear coefficient of thermal expansion, initial uniaxial yield stress);
- type of the uniaxial stress–strain curve (bilinear, nonlinear).

2. General Equations

In the following the basic equations of the analytical analysis are summarized.

Let us take the simplest form of the shrink fit: two thin disks are mechanically assembled and then thermally loaded. The inner part is the shaft of radii a and b, the outer part is the hub of radii b and c, respectively. The initial interference between shaft and hub disappears through the mounting process and, consequently, it causes an initial joint pressure p_{b0}. If the thermal loading is a steady-state, homogeneous heating, then four types of deformation are possible (KOVÁCS, 1992):

1. elastic shaft — elastic hub;
2. elastic–plastic shaft — elastic hub;
3. elastic shaft — elastic–plastic hub;
4. elastic–plastic shaft — elastic–plastic hub.

In the Case 4 the plastic zones appear at the inner side of the disks (*Fig. 1*). Using the dimensionless geometrical parameters $R = r/b, \xi_i = x_i/b, \xi_a = x_a/b$, the following equations hold:

$$\frac{\mathrm{d}\sigma_r}{\mathrm{d}R} = \frac{\sigma_t - \sigma_r}{R}, \tag{1}$$

$$\epsilon_r = \frac{\mathrm{d}U}{\mathrm{d}R}, \qquad \epsilon_t = \frac{U}{R}. \tag{2a-b}$$

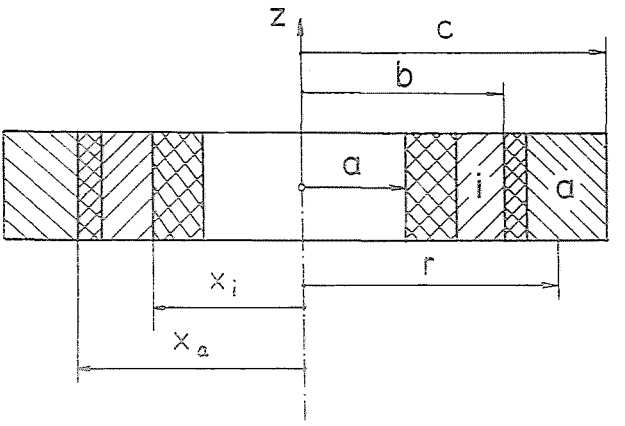

Fig. 1. Assembled shrink fit

The first equation is the equilibrium equation in the radial direction, where σ_r, σ_t are the radial and circumferential stresses, respectively. The second couple of equations expresses the geometrical relations between the radial strain ϵ_r, the circumferential strain ϵ_t and the dimensionless radial displacement $U = u/r$. The total strains are decomposed into an elastic and a plastic part:

$$\epsilon_r = \epsilon_r^e + \epsilon_r^p, \qquad \epsilon_t = \epsilon_t^e + \epsilon_t^p, \qquad \epsilon_z = \epsilon_z^e + \epsilon_z^p. \tag{3a-c}$$

Two types of constitutive equations are valid: for the elastic parts of the strains the Hooke's law holds, that is

$$\epsilon_r^e = \frac{1}{E}(\sigma_r - \nu\sigma_t) + \alpha\vartheta, \tag{4}$$

$$\epsilon_t^e = \frac{1}{E}(\sigma_t - \nu\sigma_r) + \alpha\vartheta. \tag{5}$$

whereas for the plastic parts the validity of the Tresca yield condition is assumed, that is

$$\sigma_1 - \sigma_3 = Y. \tag{6}$$

Considering perfectly elastic assemblage, the yield rule associated to the above yield condition reads

$$\epsilon_1^p + \epsilon_2^p + \epsilon_3^p = 0, \tag{7}$$

$$\epsilon_1^p \geq 0, \qquad \epsilon_2^p = 0, \qquad \epsilon_3^p \leq 0. \tag{8a-c}$$

In the above formulae $\vartheta = T - T_0$ represents the temperature (T_0 is reference temperature), the subscripts 1, 2, 3 show the conventional principal directions. Denoting the inner and outer disks by the subscript i and a, respectively, we can attach the following boundary and continuity conditions to the above equations:

$$\sigma_{ri}(q_i) = 0, \tag{9}$$

$$[\overline{\epsilon}^p(\xi_i) = 0], \tag{10}$$

$$[\sigma_{ri}(\xi_i - 0) = \sigma_{ri}(\xi_i + 0)], \tag{11}$$

$$[\sigma_{ti}(\xi_i - 0) = \sigma_{ti}(\xi_i + 0)], \tag{12}$$

$$[U(\xi_i - 0) = U(\xi_i + 0)], \tag{13}$$

$$\sigma_{ri}(1) = -p_b, \tag{14}$$

$$|\epsilon_{ti}(1) - \epsilon_{ta}(1)| = i_0/b, \tag{15}$$

$$\sigma_{ra}(1) = -p_b, \tag{16}$$

$$[\overline{\epsilon}^p(\xi_a) = 0], \tag{17}$$

$$[\sigma_{ra}(\xi_a - 0) = \sigma_{ra}(\xi_a + 0)], \tag{18}$$

$$[\sigma_{ta}(\xi_a - 0) = \sigma_{ta}(\xi_a + 0)], \tag{19}$$

$$[U(\xi_a - 0) = U(\xi_a + 0)], \tag{20}$$

$$\sigma_{ra}(q_a) = 0, \tag{21}$$

where $q_i = a/b$ and $q_a = c/b$ are dimensionless radii of the disks, p_b is the actual (temperature-dependent) joint pressure and i_0 denotes the initial interference between shaft and hub. The equations in brackets only hold in the plastic zones. The solution of the above equations gives the final joint pressure p_{b1} and the stress distributions after the thermal loading. The detailed results can be found in LIPPMANN (1992). (elastic–perfectly plastic case) and in KOVÁCS (1991). (elastic-plastic isotropic hardening case). We assume that thermal unloading only causes elastic deformation, therefore the residual stress state can be obtained by superposition (BLAND, 1956) as

$$\sigma_{r2} = \sigma_{r1} + \Delta\sigma_r, \tag{22}$$

$$\sigma_{t2} = \sigma_{t1} + \Delta\sigma_t, \tag{23}$$

where subscripts 1 and 2 refer to the thermally loaded and unloaded state, respectively, and $\Delta\sigma_r$ and $\Delta\sigma_t$ are the elastic stresses due to a joint pressure $-\Delta p_b$ calculated from the temperature elevation $-\vartheta$ using the same equations as above.

Table 1
Geometrical and material parameters

	$q_{i,a}$	E [GPa]	Y_0 [MPa]	ν	$\alpha \cdot 10^5$ [1/K]
Shaft	0.7	69	280	0.33	2.4
Hub	1.2	210	430	0.29	1.2

3. Numerical Comparison

In order to compare the effects varying the features mentioned in the Introduction, as model an aluminum–steel disk couple has been chosen. The mechanical properties are listed in *Table 1.*

In the numerical calculation, ten axisymmetric elements were used radially, (5 in the shaft, 5 in the hub, respectively) and 1 element axially. The assemblage was modeled by three node-to-line gap elements at the contacting surface. First, the initial stress-state has been calculated by vanishing the given initial interference ($i_0/b = 0.003$) as a static loading (elastic analysis). The loading path has been later accomplished by the temperature elevation (elastic-plastic analysis) and finally by the elastic unloading.

The initial joint pressure was $p_{b0} = 45.9$ MPa and the thermal cycle consisted of a heating from $\vartheta_0 = 20°C$ up to $\vartheta_1 = 180°C$ and then, of a cooling down to room temperature. The comparison of the stress distributions has been made on the final (i. e. unloaded) state.The yield stress depends on the temperature. This relation was approximated linearly by (LIPPMANN, 1992)

$$Y(\vartheta) = Y_0 - m\vartheta. \tag{24}$$

$m_i = 0.22$ [MPa/K], $m_a = 0.16$ [MPa/K] (FAUPEL and FISCHER, 1981). The temperature dependence of E and α is given in *Table 2.* The actual values were interpolated.

Table 2
Temperature dependence of material parameters

°C	20	50	100	150	200
E_i [GPa]	70	66	62	58	54
E_a [GPa]	210	210	208	205	200
α_i [*10^5 °C]	–	–	2.4	–	2.5
α_a [*10^5 °C]	–	–	1.2	–	1.28

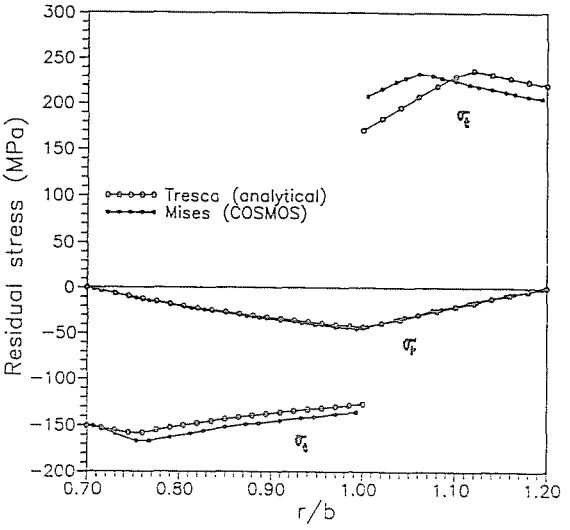

Fig. 2. Comparison of yield criteria

Fig. 2 shows the comparison of the yield criteria by using an elastic–perfectly plastic model. The radial stresses are practically the same. The hoop stresses slightly differ from each other, mainly in the outer part. The relative difference between the elastic–plastic radii ξ_i, ξ_a (break points on the hoop stress curves) is less than 1% in the inner part and about 5% in the outer part, respectively.

In the legend of the Figure 'COSMOS' refers to the commercial finite element code.

Fig. 3 shows the comparison of hardening effects. 'FEM' refers to a finite element program developed by the author (KOVÁCS, 1994b). In all cases the Mises yield condition was used. It is obvious from the diagram that hardening does not modify the results. However, it must be remarked that the greatest equivalent plastic strain did not exceed $5\,10^{-4}$. If the uniaxial stress–strain curve is nonlinear (i.e. the elastic–plastic interface is a third order polynomial, we get almost exactly the same stress distributions (see *Fig. 4*).

The largest deviation has been got by using temperature dependent material parameters (*Fig. 5*). Temperature diminishes the elasticity modulus E, therefore, the material has a larger elastic capacity — the deformation was pure elastic. The linear coefficient of thermal expansion α becomes slightly larger at higher temperature, which implies larger thermal strains and, consequently, larger stresses — the deformation is elastic-plastic. If all three parameters (E, α, Y) are temperature dependent, the contrary ef-

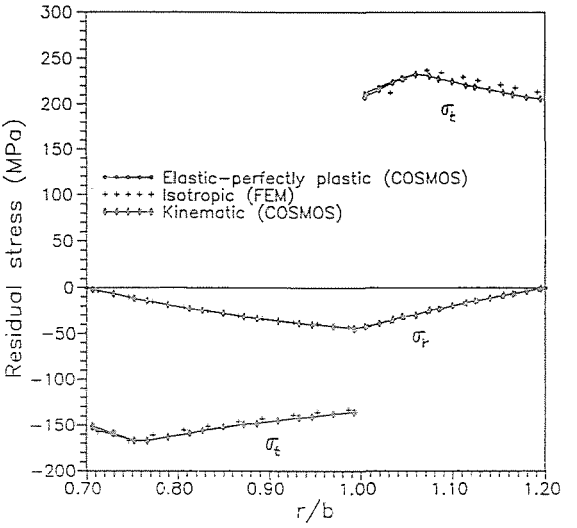

Fig. 3. Comparison of hardening effects

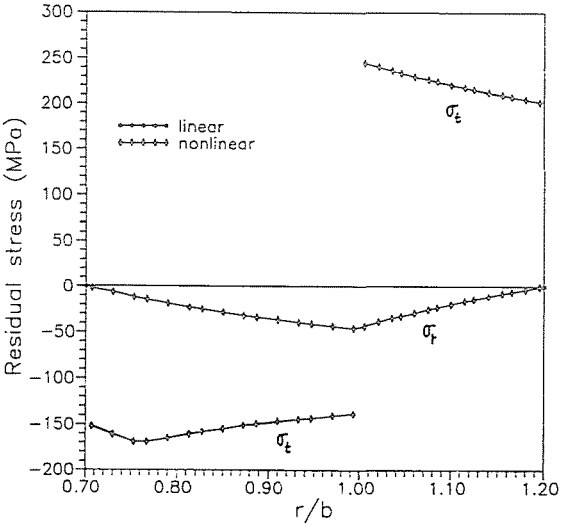

Fig. 4. Stress distributions by different stress–strain curves

fects result elastic–plastic deformation in the shaft and pure elastic deformation in the hub. Although the hoop stress distributions are different, the radial stresses are practically the same.

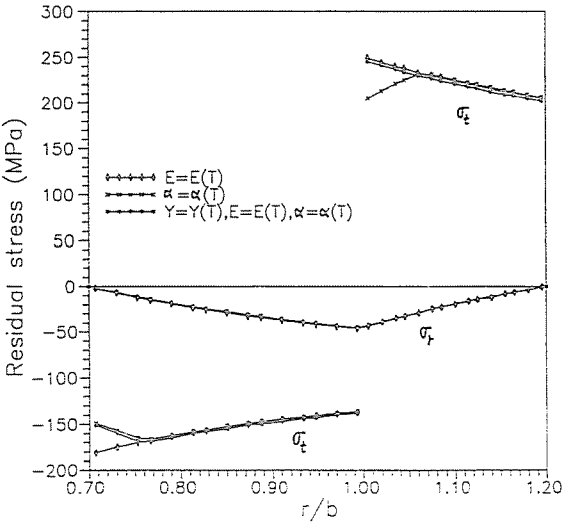

Fig. 5. Residual stresses by temperature dependent parameters

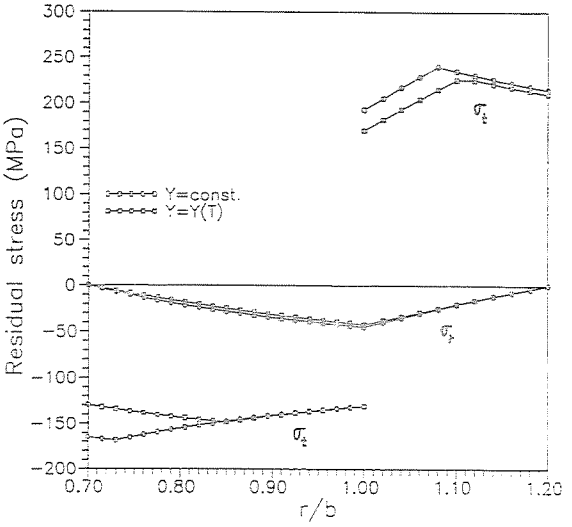

Fig. 6. Residual stresses by temperature dependent yield stress

Taking into consideration the temperature dependence of the yield stress, the effect is similar to that of α, however, the amount of deviation was much larger: at the original temperature elevation the fit fully plastified. *Fig. 6* shows the results by less thermal load, where the maximum temperature

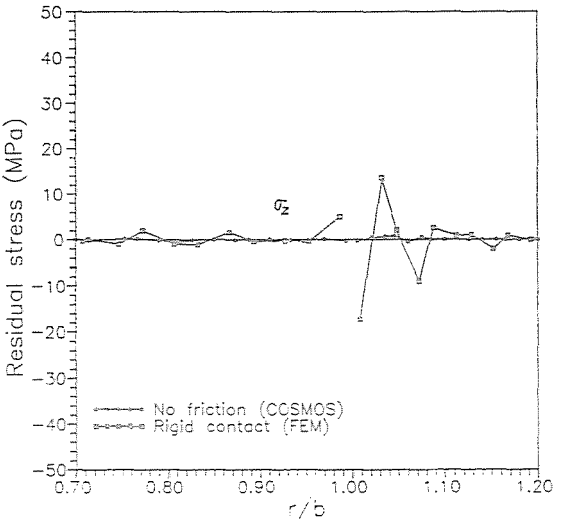

Fig. 7. Effect of friction on the axial stress distribution

was $\vartheta_1 = 160°C$. The relative difference between the elastic–plastic radii ξ_i is more than 10% in the shaft.

The effect of friction is shown in *Fig. 7.* By rigid contact the axial stress becomes large enough near the joint, in the order of the radial stress. However, this relative large axial stress does not modify the radial stress distribution. The stress jump at the joint is due to the rigid contact. The oscillation near the joint can be explained by the small number of finite elements. This selection has been described accurately enough the radial and hoop stress distribution. however, it caused the unrealistic oscillation here.

4. Summary

The extreme deviations of the results were the following:

- The minimum residual joint pressure was by about 6% less than the initial one, the maximum was equal to it (in pure elastic deformation).
- The difference between the smallest and largest dimensionless plastic radii happened to be 14% in the inner part and 20% in the outer part of the fit.
- Exceptional deformations occurred by using temperature dependent elastic modulus, when there was only elastic deformation, and by using temperature dependent yield stress, when there was full plastic

deformation detected. The latter case would mean a plastic collapse, making impossible the load transmission.

Concluding the numerical calculations, we obtained that the residual radial stress distribution, which explicitly affects the joint pressure, remained almost the same by changing the mechanical model. The temperature dependence of material properties essentially modified the hoop stress distributions — the most sensitive parameters are E and Y. The shape of more realistic stress-strain curve is indifferent in the range of possible plastification. The fit fully plastifies much sooner than the effect of nonlinearity could be detected. Friction mainly affects only the axial stresses near the joint.

References

BLAND, D. R. (1956): Elasto-plastic Thick-walled Tubes of Work-hardening Material subject to Internal and External Pressures and to Temperature Gradients. *J. Mech. Phys. Solids*, Vol. 4, pp. 209–229.

FAUPEL, J. H. - FISCHER, F. E. (1981): Engineering Design. John Wiley & Sons, New York.

GAMER, U. - LANCE, R. H. (1982): Elastisch-plastische Spannungen im Schrumpfsitz. *Forsch. Ing.-Wes.*, Vol. 48, pp. 192–198.

KOLLMANN, F. G. (1978): Die Auslegung elastisch-plastisch beanspruchter Querpreßverbände. *Forsch. Ing.-Wes.*, Vol. 44, pp. 1–11.

KOLLMANN, F. G. – ÖNÖZ, E. (1983): Ein verbessertes Auslegungsverfahren für elastisch-plastisch beanspruchte Preßverbände. *Konstruktion*, Vol. 35, pp. 439–444.

KOVÁCS, Á. (1991): Hardening Effects on the Stress Distribution in a Shrink Fit under Cyclic Thermal Loading. *Periodica Polytechnica Ser. Mech. Eng.*, Vol. 35, No. 1–2, pp. 49–64.

KOVÁCS, Á. (1992) : Analytische und numerische Berechnungen von Wärmespannungen in Schrumpfverbänden. *Technical Report*, TU München, Lehrstuhl A für Mechanik.

KOVÁCS, Á. (1994a): Thermal Stresses in a Shrink Fit due to an Inhomogeneous Temperature Distribution. *Acta Mechanica*, Vol. 105, pp. 173–187.

KOVÁCS, Á. (1994b): Thermoelastic-plastic Deformations of Shrink Fits. *ZAMM*, Vol. 74, No. 4, pp. T310–T312.

LIPPMANN, H. (1992) : The Effect of a Temperature Cycle on the Stress Distribution in a Shrink Fit. *Int. J. Plasticity*, Vol. 8, pp. 567–582.

MACK, W. (1986): Spannungen im thermisch gefügten elastisch-plastischen Querpreßverband mit elastischer Entlastung. *Ing.-Arch.*, Vol. 56, pp. 301–313.